Nighttime vertical plasma drifts and the occurrence of sunrise undulation at the dip equator: A study using Jicamarca incoherent backscatter radar measurements

K. M. Ambili,[1] R. K. Choudhary,[1] J.-P. St.-Maurice,[2] and Jorge L. Chau[3]

Received 26 September 2013; accepted 16 October 2013; published 11 November 2013.

[1] The absence of photoionization, in combination with sustained downward plasma motion at night, means that the *F* region can be severely depleted at the magnetic equator in the morning. As a result, at sunrise, there can be a sudden upward jump in altitude of the *F* region peak followed by a quick descent in association with the downward motion of the photoionization production peak. This constitutes what is known as the equatorial sunrise undulation. Its anecdotal existence has been reported over Jicamarca while it has been seen repeatedly over Trivandrum, India, during equinox conditions. By contrast, we find that the phenomenon is not as frequent at Jicamarca as at Trivandrum. Using incoherent backscatter radar data from Jicamarca, we show that the differences have an electrodynamical origin. The sunrise undulation gets masked when remnant plasma from the previous night does not move down to low enough altitude. The nighttime residual ion density and its altitude are found to be strongly influenced by the evening and nighttime electric field. There is a strong association between a strong plasma uplift at sunset and the appearance of an undulation at sunrise around the magnetic equator. **Citation:** Ambili, K. M., R. K. Choudhary, J.-P. St.-Maurice, and J. L. Chau (2013), Nighttime vertical plasma drifts and the occurrence of sunrise undulation at the dip equator: A study using Jicamarca incoherent backscatter radar measurements, *Geophys. Res. Lett.*, *40*, 5570–5575, doi:10.1002/2013GL057837.

1. Introduction

[2] At sunrise around the dip equator, the altitude of the *F* region peak density (hmF_2) can undergo a quick upward motion ahead of an equally rapid downward motion [*Balsley*, 1969; *Woodman*, 1970; *Aggson et al.*, 1995]. This phenomenon has been called the sunrise oscillation [*Ambili et al.*, 2012], though a more precise term should really be the "sunrise undulation" (SU). It was initially proposed that this phenomenon was the result of an electrodynamic phenomenon [*Woodman*, 1970; *Aggson et al.*, 1995], in analogy to the well known evening prereversal enhancement in the electric field [*Fejer*, 1981; *Scherliess and Fejer*, 1999]. The plasma was believed to be pushed down by a westward electric field before being pushed upward after sunrise when the zonal equatorial electric field turned eastward. However, *Ambili et al.* [2012] have shown that the undulation is actually the product of photochemistry rather than electrodynamics. Newly created plasma at sunrise follows a quick downward motion imposed by the rate of photoionization which becomes stronger and moves lower down as the solar zenith angle undergoes its rapid decrease at sunrise. This stated, electrodynamics was shown to still play an important, though indirect, role by pushing remnant plasma from the previous night down in altitude so as make it undergo substantial recombination by the end of the night. The undulation was the result of a replacement of a low altitude low density plasma by more abundant newly created plasma first appearing at higher altitudes. Thus, the value and peak altitude of the remnant plasma density just before sunrise is central to the detection of an undulation and this remnant density does depend on the history of the electric field during the previous night. Therefore, longitudinal differences in the background zonal electric field [*Scherliess and Fejer*, 1999] could play an important role in the occurrence of the hmF_2 SU's. For this reason, we have studied the phenomenon at Jicamarca with an eye on its possible dependence on the electric field during the previous night, the idea being that the evening Pre Reversal Enhancement (PRE) in the electric field, equatorial spread F during the night and the SU could all be connected.

[3] Our initial focus for this study was equinoctial months since the SU frequency of occurrence is very high at that time of year at Trivandrum [*Ambili et al.*, 2012]. We anticipated a similar strong effect at Jicamarca given that we expected similar background conditions during equinox at Jicamarca [*Fejer*, 1981]. An added advantage of Jicamarca is that detailed *F* region electron densities can be extracted from an on-site incoherent scatter radar if the radar is turned on. Also, digisonde observations are routinely available there. However, the SU turned out to be less frequent at Jicamarca compared to Trivandrum. To study the reasons for this, we identified two events for which incoherent scatter radar (ISR) data were available to help shed light on the situation. One of these was for a typical equinoctial day. The other took place during a geomagnetically disturbed day. As shown below, our detailed study of these events revealed that the differences had an indirect electrodynamical origin.

2. Data and Method of Analysis

[4] The *F* region electron density information at Jicamarca (12°S, 76.9°W, 1.7°S dip latitude) was retrieved

[1]Space Physics Laboratory, Vikram Sarabhai Space Centre, Trivandrum, India.
[2]Institute of Space and Atmospheric Studies, University of Saskatchewan, Saskatoon, Saskatchewan, Canada.
[3]Leibniz Institute of Atmospheric Physics, Rostock University, Kuhlungsborn, Germany.

Corresponding author: R. K. Choudhary, Space Physics Laboratory, Vikram Sarabhai Space Centre, Trivandrum, Kerala 695 022, India. (rajkumar_choudhary@vssc.gov.in)

0094-8276/13/10.1002/2013GL057837

from a Digital Portable Sounder (DPS), or "digisonde", and, sometimes, from the ISR. The Digisonde sweeps frequencies in the range 1–30 MHz and provides reliable estimates for the electron density below the *F* region peak through the "true height inversion algorithm" [*Reinisch et al.*, 2009]. The Digisonde scaled parameters were downloaded from the Jicamarca database (*http://digisonde.igp.gob.pe*).

[5] The Jicamarca ISR operates at 49.92 MHz. It has a large square array of 18,432 half-wave dipoles arranged into 64 separate modules of 12 x 12 crossed half-wave dipoles. Each module has a beam width of about 7°, and the array can be steered within this region by proper phasing providing the two way half power beam width of the order as low as 0.8°. More technical details on the Jicamarca radar are given in *Woodman* [1970].

[6] We compared measurements from the Jicamarca digisonde and/or ISR with calculations from a numerical time-dependent model that solves the electron and ions continuity equations [*Ambili et al.*, 2012]. Being only interested in the 100 to 500 km altitude range, we limited the calculation to the O^+, O_2^+, N_2^+, and NO^+ ions. The model includes photoionization of O, N_2, O_2, conversion of O^+ to molecular ions by charge exchange reactions and dissociative recombination of the latter. The model also includes the photoproduction of atomic oxygen ions into metastable such as $O^+(2D)$ and $O^+(2P)$ and incorporates the relevant chemical reactions of those metastable states [*Richards*, 2011]. Ionization from photoelectrons was also added for the lower altitudes using the scheme proposed by *Richards and Torr* [1988].

[7] The model includes the effects of transport from vertical electrodynamic drifts associated with zonal electric fields [*Choudhary et al.*, 2011], but it does not include diffusion and the horizontal transport of plasma. The *F* region peak (hmF_2) being below 400 km, the magnetic field lines are still very horizontal, and the time scale for diffusion to operate is much longer than the time scales of interest for the present work: consider the diffusion equation along the magnetic field when the gravitational field is vertical and the magnetic field is horizontal at the magnetic equator. We then have

$$\frac{\partial n}{\partial t} = \frac{KT_p}{m\nu}\frac{\partial^2 n}{\partial s^2} \tag{1}$$

where K, m, T_p, and ν, are the Boltzmann's Constant, mass, plasma temperature, and ion-neutral collision frequency, respectively. s is along the geomagnetic field lines (horizontal at the dip equator) while $T_p = (T_e + T_i)/2$. From dimensional analysis, the gradient scale, Δs, is given by

$$(\Delta s) = \sqrt{\frac{KT_p}{m\nu}\Delta t} \tag{2}$$

Using $KT_p/m \approx 1400^2\ m^2/s^2$ for O+ ions at 1000 K for T_i and for T_e (probably an upper estimate for the situation at hand) and using $\nu \approx 0.5 s^{-1}$ at the upper altitudes of interest (larger values from lower down would imply that smaller gradient scales would be involved), we get $\Delta s \approx 2800\sqrt{\Delta t}$. As sunrise is a fast evolving phenomenon, Δt should be of the order of 10 min or less for transport effects to have time to be felt. This means gradient scales of the order of 70 km. However, the field lines at the magnetic equator are horizontal over 200 km scales and the gradient scales should therefore be well in excess of 200 km, not to mention that 10 min is really too long a time scale. Therefore, for a phenomenon where dramatic changes occur over a 10 min scale, transport along the magnetic field will not contribute if the apex of a field line is below 400 km altitude. Equivalently, we can compute the time scale over which transport would contribute. Using the same parameters as above but assuming a very conservative gradient scale of 200 km, we find

$$\Delta t = \frac{\nu}{KT/m}(\Delta s)^2 \approx \frac{0.5 \times (200 \times 10^3)^2}{1400^2} = 10^4 s \tag{3}$$

This is of the order of 2.5 h, which is too long. This still leaves meridional neutral wind effects as a final potential candidate to affect the calculations of the SU. However, for meridional winds to have an influence, the plasma would have to be carried over a scale of 100 km in a time well less than 30 min, requiring meridional winds well in excess of 50 m/s. Such winds are not expected at the equator, at least on average [*Emmert et al.*, 2008].

3. Results and Discussion

3.1. The Jicamarca SU and Its Connection With Spread F

[8] Figure 1 describes the temporal variations in the Jicamarca digisonde-derived hmF_2 during the time interval between 0400 and 0700 LT and between 1800 to 2400 LT at very different times of the year, namely, during the winter solstice (June 2010, left panels), summer solstice (December 2010, middle panels), and at equinox (March 2011, right panels). These plots represent monthly averaged values at 15 min intervals along with standard deviations.

[9] The Figure clearly shows that there is an association between the evening behavior of the plasma and the morning undulation. In particular, when the hmF_2 is high at midnight (December), there is no SU to be seen. Conversely when the *F* region hardly moves upward in the evening (June), the SU is particularly clear. When the hmF_2 in the evening rises to a high altitude in early evening and falls off quickly by midnight (March), we have a mixed case where the SU is detectable but not as clean as for June.

[10] The characteristic behavior of the hmF_2 in the evening is nicely explained by the statistics on the vertical drifts during the same time period. This can be seen from the rightmost panel in Figure 1, where we plotted the monthly averaged values of V_z between 1800 and 2400 LT for Jicamarca. These values were obtained from the Fejer model [*Scherliess and Fejer*, 1999] rather than ISR measurements for the period of interest as there were no sufficient ISR drift measurements during this period to get a properly averaged monthly behavior. This stated, the model and ISR measurements at Jicamarca are known to agree well [*Scherliess and Fejer*, 1999]. In this light, Figure 1 shows that the PRE in the vertical drift is strong during equinox and that, moreover, the hmF_2 is much higher in the evening when the plasma drift is upward and large. Also, in December, the vertical drift does not start as intense as in March but the downward drift for most of the evening remains weaker until midnight meaning that the plasma is not pushed downward very hard after 2000 LT. This explains the rather high altitude of the hmF_2 by midnight compared with the other periods.

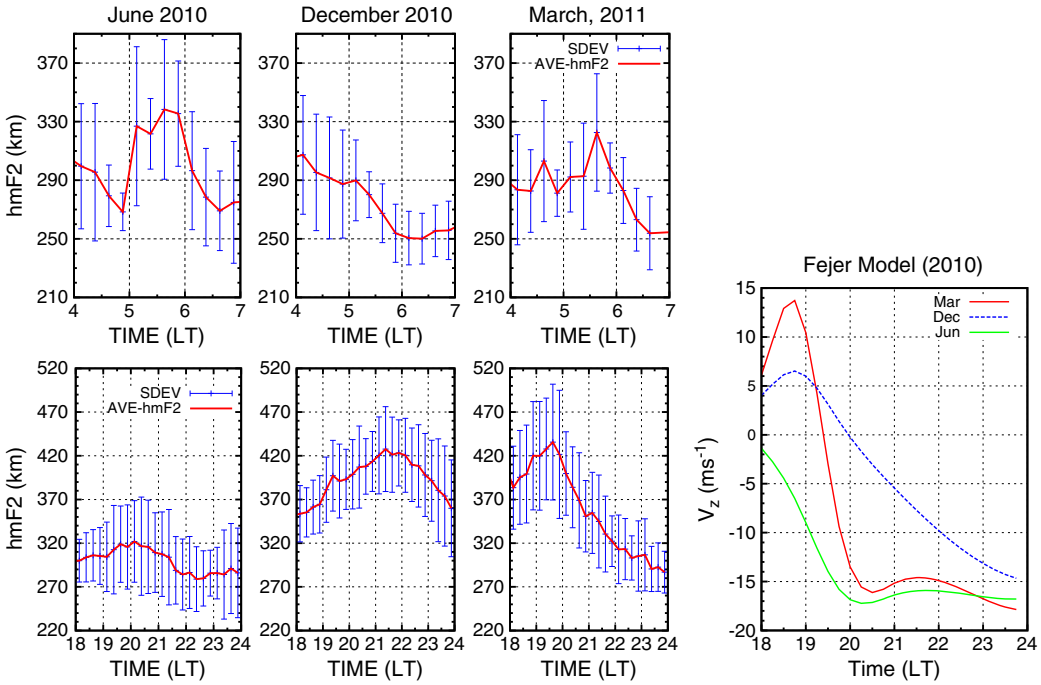

Figure 1. Temporal variations in the average value of hmF_2 in 15 min intervals along with standard deviations obtained using observations from a Digisonde at Jicamarca during sunrise hours (top panels) and sunset hours (bottom panels) for the winter solstice (June, left panels), summer solstice (December, middle panels), and equinox (March, right panels). Rightmost panel: model V_z values at Jicamarca for the same three months of the year.

[11] While we can conclude from the above that there is a connection between a lack of plasma uplift in the evening and the occurrence of a SU, another connection is seen with the occurrence of equatorial spread F (ESF), which, in the Peruvian sector, maximizes during March and December while being a minimum during June [*Rastogi*, 1980; *Fejer*, 1981]. A strong PRE is known to be related to ESF, most likely because the plasma is more unstable when the *F* peak is higher [*Fejer et al.*, 1999]. For example, in December, when ESF occurs over 90% of the nights in the Peruvian sector, the hmF_2 remains high for the whole evening period. This in turn can be explained from the vertical drift pattern.

3.2. *F* Region Ionization Remnants and the SU

[12] While we can establish a clear connection between the SU and the electrodynamics of the previous evening, the mechanism responsible for this connection needs to be clarified, given that for all three times of the year, the hmF_2 appeared to be at the same height by 0400 LT, as seen in Figure 1. To address this question, we have search the Jicamarca ISR database for events taking place at the appropriate time to allow us to more clearly assess just how remnant plasma from the previous night might be masking the sunrise effect. We found seven events, none of which exhibited a pure SU.

[13] We identified 9 September 2010 and 12 March 2011 as two suitable dates to carry out our ISR case studies. On 12 March 2011, observations from the digisonde were also available, while only ISR measurements were available on 9 September. We compared the observations with our numerical model by initializing the model under two different set of conditions, namely, (Case 1) with negligible density so that only the newly produced plasma and hence the evolution of the ionosphere with time could be tracked and (Case 2) with the plasma density matching the ISR observations at the pre-sunrise time. Having no drift data, we used the vertical drift from the Fejer drift model [*Scherliess and Fejer*, 1999] in both cases.

[14] Figure 2 compares various model calculations with the 9 September 2010, observations. The top left panel of Figure 2 represents initial conditions. The next panel to the right shows the electron density profile at 0537 LT. In this case, although the newly produced plasma peaks at 350 km (red curve), the remnant plasma density is much larger than the freshly produced one, and the hmF_2 is lower, at around 270 km. It should be clear from this alone that there will be no SU in this instance since photochemistry is not contributing much to the density so that no fast downward motion of the peak will be observed. Instead, the two curves will gently merge as time progresses owing to the stabilizing influence of the recombination with the background neutrals below 250 km. Therefore, by 06:03 LT (bottom left panel), both the newly produced plasma and the observation peak at 250 km, even though the density of newly produced plasma, is still lower than observed. After 15 more minutes, by 06:15 LT (next panel on the right), all three curves are a match near the *F* peak.

[15] To help drive the point about the importance of remnant densities for the SU, the rightmost panel of Figure 2 shows the temporal evolution of the ISR-derived hmF_2 between 03:00 and 07:00 LT and its comparison with the model-derived value. The model was initialized with a negligible background density so as to track only the fresh production of plasma. Until 0600 LT, the hmF_2 is between 250 and 270 km. The main point is to show that if the background plasma had not been present, the hmF_2 should

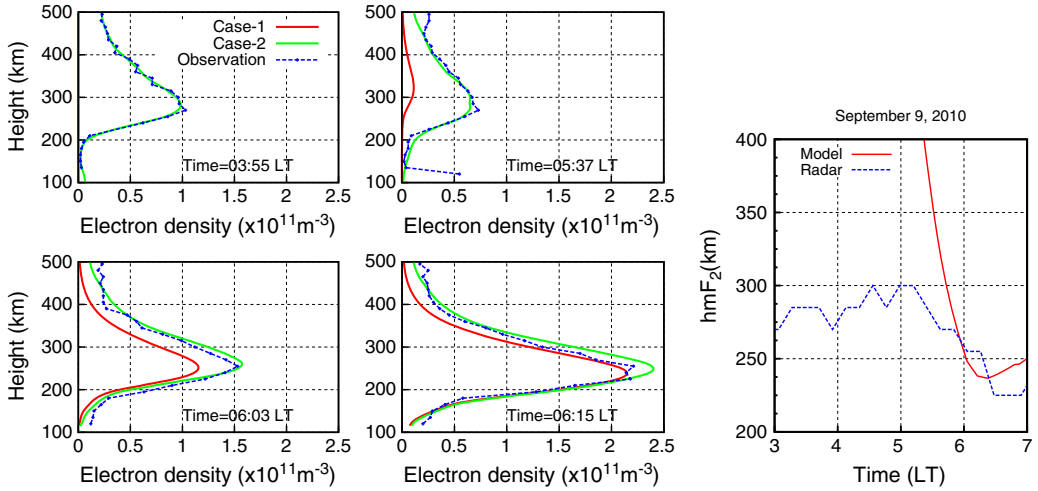

Figure 2. Comparison of model calculations with electron density observations from incoherent back scatter radar at different local times of the morning at Jicamarca on 9 September 2010. Blue traces: observations. Case 1 (red): model run with zero initial density. Case 2 (green): model run with initial density matching ISR observations at 0400 LT. In both the cases, Fejer drift was used. Rightmost panel: temporal hmF_2 evolution seen by the ISR between 0300 and 0700 LT (dotted blue line) and comparison with model-derived hmF_2 (full red line). The model for that panel was initialized with a negligible background density to track down only the fresh production of plasma. Note that where the red and green curves overlap, only the green curve is seen.

have been higher, as shown by the red curve in the plot. After 0615 LT, as the freshly produced plasma dominates, the hmF_2 matches the model output which tracks the F peak associated only with photoionization.

[16] It is also interesting to note that at any time between 0400 and 0600 LT on 9 September 2010, the ISR does not indicate a double peak in the electron density profile, as previously suggested by *Ambili et al.* [2012]. The reason for the nonappearance of a double peak structure rests with the remnant plasma from the night before, which is present at all heights up to 500 km even though the density peaks only at 300 km. In this case, the density of newly produced plasma is simply much less than that of the remnants for those altitudes. Nevertheless, we now show an example of double peak seen on 12 March 2011, during a geomagnetically disturbed day.

3.3. Double Hump Structure in the Electron Density Profile

[17] The double peak in the electron density profile on 12 March 2011 happened after a moderate geomagnetic storm with Dst $\approx$ -90 nT had started on 11 March 2011 at 0300 UT and was in its recovery phase on 12 March. In the early morning hours of 12 March at Jicamarca, both the digisonde and incoherent backscatter radar observed an upward movement in the hmF_2 from around 300 km at 0400 LT to 400 km at 0600 LT (UT-0600). The plasma only came down to 250 km by 0700 LT. The high altitude of the F peak shortly before sunrise was unusual, as the hmF_2 usually steadily moves down at that time of day, owing to a background westward zonal electric field. In the 12 March case, however, the zonal field was eastward, most likely due to the overshielding of the magnetosphere [*Stern*, 1975]. Such a situation is fairly common at the dip equator during the recovery phase of a geomagnetic storm [*Huang et al.*, 2005].

[18] There were no good observations from either the digisonde or the ISR during the interval 0400 to 0600 LT, as the data were contaminated by ESF echoes, also known to occur in the postmidnight period during geomagnetic disturbed conditions [*Fejer et al.*, 1999; *Hysell and Burcham*, 2002]. It also resulted in data gap in Figure 3 between 04:00 and 06:00 LT. The late night ESF phenomenon is associated with the anomalous reversals of the nighttime drifts from downward to upward [*Fejer et al.*, 1999] which makes the bottomside of the F layer unstable when high enough. The presence of ESF only goes to confirm that the electric field was eastward during the interval 0400 to 0600 LT on 12 March providing indirect evidence that the hmF_2 was indeed higher than usual during the data gap.

[19] In large part owing to the ISR density data, Figure 3 shows what was really happening during the early morning hours on 12 March 2011. In the rightmost panel, we see how the hmF_2 was going up until 0400 LT, at which point the ESF-related data gap took place for 2 h. Notice how there was no data available at the time the SU was to take place (red trace in rightmost panel). The other panels show that when the data first reappeared, well after sunrise, the F region plasma had two peaks separated by almost 200 km in altitude. As the Fejer model output could not represent actual electric field conditions prevailing during special events like on 12 March in our model run for Case 2, we initialized the model with ISR-measured plasma density at 03:00 A.M. and applied a modest updrift of 5 m/s till 06:15 LT (there was no drift data from the ISR itself). Afterward, we used the Fejer drift in the calculations. While the agreement with observations may not be perfect, our model calculations can clearly be used to emphasize that the lower peak in the density profile was associated with the SU effect while the other peak came from remnant plasma that had been lifted up to unusually high altitudes and had undergone little, if any, recombination. This upper peak descended near dawn because of the downward motion seen after 0615 LT. The motion of the upper peak therefore had nothing to do with the chemical processes associated with the plasma produced

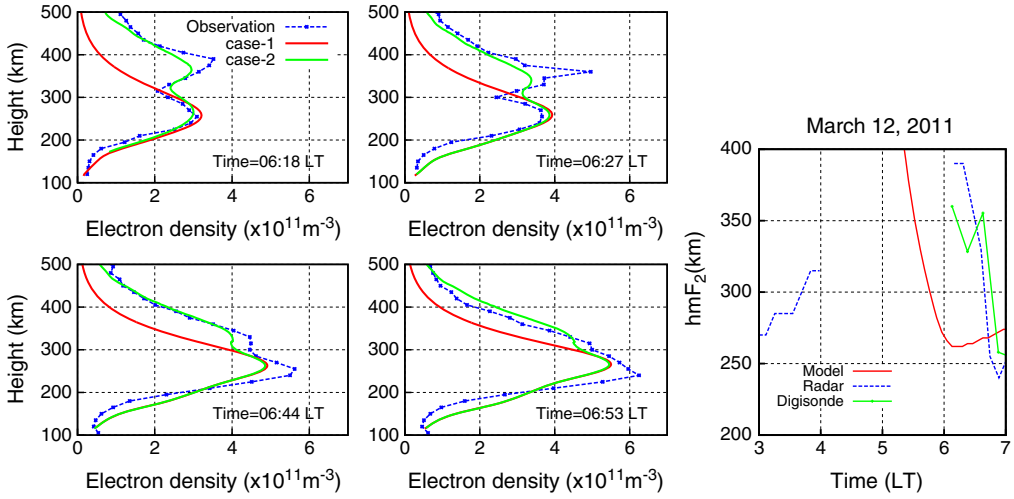

Figure 3. Same as Figure 2 but for 12 March 2011. In Case 2 (green curve), the model was initialized with the density at 03:00 A.M. and a drift of 5 m/s was applied till 06:15 A.M. after which Fejer model derived drift was used.

through the SU mechanism. It just so happened that the remnant plasma was high enough and had a large enough density to be seen in tandem with the photochemically produced plasma, even as late as 0653 LT. Therefore, even though there was an initial rise in altitude followed by a downslide after sunrise, the temporal variations in hmF_2 on 12 March 2011 was entirely due to an unusual electrodynamical effect.

4. Conclusion

[20] In the light of the above discussion, it becomes easier to understand seasonal variations in the sunrise undulation (SU) presented in Figure 1. During equinox (March and September) and summer solstice months (i.e., December), the SU is not so frequent because of relatively higher background remnant plasma densities near sunrise. We found this to be related to the enhanced PRE electric field in the evening, which pushes the plasma up in altitude and often causes ESF by the same token. As a result of the upward push in the evening, there is enough background remnant plasma density around sunrise to mask the sunrise chemical production effect that gives rise to the SU. We then only see a downward motion of the F peak in the morning, until the plasma reaches 250 km, where recombination stops the downward motion of the F region, allowing photochemistry to take over. By contrast, during the June solstice, PRE events are far less frequent and/or weaker, causing the plasma to stay at low altitudes in the evening. The background westward field during the night is therefore able to push the plasma down into the regions where recombination dominates. In that case, since the background remnant plasma density is low, the SU can clearly be seen.

[21] Our study also makes it clear that the altitude of the remnant plasma is important, not just its magnitude. The 12 March 2011 example provided an example in which the background plasma was pushed quite far up in altitude after a strong eastward electric field occurred an hour before sunrise, as a result of a magnetic storm. In that case, an apparent SU was observed but the physics was actually different and the details of the undulation were different, being in effect of an electrodynamic rather than chemical nature. In particular, the ISR showed that there was even a double-hump density structure in the F region plasma, with the remnant plasma providing a peak that was much higher than normal. It is important to note that all the digisonde would have been able to see in this case was a sunrise-like undulation in the temporal variations of F region peak height since only one density peak would have been visible to it. This is something to beware of, as ionosondes provided most of the SU data through their operation on a day-to-day basis and their large number of locations.

[22] We conclude that the background density plays a determinant role in the observation of a SU in the F region peak and that this background density is quite sensitive to the electric field between sunset and sunrise. Given that there can be important longitudinal differences in the electric field at the geomagnetic equator, this explains the large variability in the occurrence of the SU at different locations.

[23] **Acknowledgments.** The Jicamarca Radio Observatory is a facility of the Instituto Geofisico del Peru operated with support from the NSF AGS-0905448 through Cornell University. The help of Simi R.S. in data analysis is gratefully acknowledged. KMA was supported by an ISRO Research Fellowship during the tenure of this work.

[24] The Editor thanks one reviewer for assistance evaluating this manuscript.

References

Aggson, T. L., F. A. Herrero, J. A. Johnson, R. F. Pfaff, H. L. Kso, N. C. Maynard, and J. J. Moses (1995), Satellite observations of zonal electric fields near sunrise in the equatorial ionosphere, *J. Atmos. Terr. Phys.*, *57*(1), 19–24.

Ambili, K. M., J.-P. St.-Maurice, and R. K. Choudhary (2012), On the sunrise oscillation of the F region in the equatorial ionosphere, *Geophys. Res. Lett.*, *39*, L16102, doi:10.1029/2012GL052876.

Balsley, B. B. (1969), Some characteristics of non-two-stream irregularities in the equatorial electrojet, *J. Geophys. Res.*, *74*, 2333–2347.

Choudhary, R. K., J. P. St.-Maurice, K. M. Ambili, S. Sunda, and B. M. Pathan (2011), The impact of the January 15, 2010, annular solar eclipse on the equatorial and low latitude ionospheric densities, *J. Geophys. Res.*, *116*, A09309, doi:10.1029/2011JA016504.

Emmert, J. T., et al. (2008), DWM07 global empirical model of upper thermospheric storm-induced disturbance winds, *J. Geophys. Res.*, *113*, A11319, doi:10.1029/2008JA013541.

Fejer, B. G. (1981), Low latitude electodynamic plasma drifts: A review, *J. Atmos. Terr. Phys.*, *53*, 677–693.

Fejer, B. G., L. Scherliess, and E. R. de Paula (1999), Effects of the vertical plasma drift velocity on the generation and evolution of equatorial spread F, *J. Geophys. Res.*, *104*, 19,859–19,870, doi:10.1029/1999JA900271.

Huang, C.-S., J. C. Foster, and M. C. Kelley (2005), Long-duration penetration of the interplanetary electric field to the low-latitude ionosphere during the main phase of magnetic storms, *J. Geophys. Res.*, *110*, A11309, doi:10.1029/2005JA011202.

Hysell, D. L., and J. D. Burcham (2002), Long term studies of equatorial spread F using the JULIA radar at Jicamarca, *J. Atmos. Sol. Terr. Phys.*, *64*, 1531–1543, doi:10.1016/S1364-6826(02)00091-3.

Rastogi, R. G. (1980), Seasonal variation of equatorial spread F in the American and Indian zones, *J. Geophys. Res.*, *85*, 722–726, doi:10.1029/JA085iA02p00722.

Reinisch, B. W., et al. (2009), New digisonde for research and monitoring applications, *Radio Sci.*, *44*, RS0A24, doi:10.1029/2008RS004115.

Richards, P. G. (2011), Reexamination of ionospheric photochemistry, *J. Geophys. Res.*, *116*, A08307, doi:10.1029/2011JA016613.

Richards, P. G., and D. G. Torr (1988), Ratios of photoelectron to EUV ionization rates for aeronomic studies, *J. Geophys. Res.*, *93*, 4060–4066.

Scherliess, L., and B. G. Fejer (1999), Radar and satellite global equatorial F region vertical drift model, *J. Geophys. Res.*, *104*, 6826–6842.

Stern, D. P. (1975), The motion of a proton in the equatorial magnetosphere, *J. Geophys. Res.*, *80*, 595–599, doi:10.1029/JA080i004p00595.

Woodman, R. F. (1970), Vertical drift velocities and east-west electric fields at the magnetic equator, *J. Geophys. Res.*, *75*, 6249–6259.